

Parameter Identification of the Nonlinear Double-Capacitor Model for Lithium-Ion Batteries: From the Wiener Perspective

Tian, N.; Fang, H.; Wang, Y.

TR2019-065 July 11, 2019

Abstract

Battery parameter identification is emerging as an important topic due to the increasing use of battery energy storage. This paper studies parameter identification for the nonlinear double-capacitor (NDC) model for Lithium-ion batteries, which is a new equivalent circuit model developed in the authors' previous work [1]. It is noticed that the NDC model has a structure similar to the Wiener system. From the Wiener perspective, this work builds a parameter identification approach for this model upon the well-known maximum a posteriori (MAP) estimation. The purpose of using MAP is to overcome the nonconvexity and local minima that can cause unphysical parameter estimates. The proposed approach is the first one that we aware of exploits MAP for Wiener system identification. It also demonstrates significant effectiveness for accurate identification of the NDC model, validated through simulations and experiments.

American Control Conference (ACC)

This work may not be copied or reproduced in whole or in part for any commercial purpose. Permission to copy in whole or in part without payment of fee is granted for nonprofit educational and research purposes provided that all such whole or partial copies include the following: a notice that such copying is by permission of Mitsubishi Electric Research Laboratories, Inc.; an acknowledgment of the authors and individual contributions to the work; and all applicable portions of the copyright notice. Copying, reproduction, or republishing for any other purpose shall require a license with payment of fee to Mitsubishi Electric Research Laboratories, Inc. All rights reserved.

Parameter Identification of the Nonlinear Double-Capacitor Model for Lithium-Ion Batteries: From the Wiener Perspective

Ning Tian, Huazhen Fang and Yebin Wang

Abstract—Battery parameter identification is emerging as an important topic due to the increasing use of battery energy storage. This paper studies parameter identification for the nonlinear double-capacitor (NDC) model for Lithium-ion batteries, which is a new equivalent circuit model developed in the authors' previous work [1]. It is noticed that the NDC model has a structure similar to the Wiener system. From the Wiener perspective, this work builds a parameter identification approach for this model upon the well-known maximum a posteriori (MAP) estimation. The purpose of using MAP is to overcome the nonconvexity and local minima that can cause unphysical parameter estimates. The proposed approach is the first one that we are aware of exploits MAP for Wiener system identification. It also demonstrates significant effectiveness for accurate identification of the NDC model, validated through simulations and experiments.

I. INTRODUCTION

Battery modeling and parameter identification are of foundational importance for model-based battery management to ensure the performance, safety and life of various battery systems. Despite a growing amount of research, many new challenges continue to arise due to an ever-increasing demand for better accuracy, efficiency and availability of battery models. In this context, this paper contributes a study of parameter identification for the nonlinear double-capacitor (NDC) model, an equivalent circuit model for Lithium-ion batteries (LiBs) proposed in our previous work [1]. Our study connects the Wiener system identification with the NDC model as the latter demonstrates a Wiener-type structure. We propose a parameter estimation approach that enhances existing Wiener identification methods and proves to be effective for the NDC model.

Literature Review. Battery parameter identification has attracted considerable attention in recent years. The current literature can be divided into two main categories, experiment-based and data-based. The first category conducts experiments of charging, discharging or electrochemical impedance spectroscopy (EIS) and utilizes the experimental data to directly determine the parameters of a model. It is pointed out in [2–4] that the transient voltage responses under constant- or pulse current charging/discharging can expose the resistance, capacitance and time constant parameters of the well-known Thevenin's model. The relationship between the state-of-charge (SoC) and open-circuit voltage (OCV)

greatly characterizes a battery's dynamics. It can be experimentally identified by charging or discharging a battery using a very small current [5], or alternatively, using a current of normal magnitude but intermittently (a sufficiently long rest period is applied between two discharging operations) [6; 7]. The EIS experiments have also been widely used to identify a battery's impedance properties [8–10]. While involving basic data analysis, methods of this category generally put emphasis on the design of experiments. By contrast, the second category seeks to deeply understand the model-data relationship and build sophisticated data-driven approaches to construct models from data. It can beneficially enable provably correct identification, even for complex models, in addition promising better use of data and convenient application. It is proposed in [11] to identifying the Thevenin's model by solving a set of linear and polynomial equations. Another popular means is to formulate model-data fitting problems and solve them using least squares or other optimization methods to estimate the parameters [12–17]. In [18; 19], a linear state-space model is formulated for batteries, and subspace identification is then performed to infer the system matrices. When more complex electrochemical models are considered, the identification usually involves large-size nonlinear nonconvex optimization problems. In this case, particle swarm optimization and genetic algorithms are often leveraged to search for the best parameter estimates [20–23]. Another topic of interest is optimal input design to maximize the parameter identifiability [24; 25].

Compared with the above studies, the NDC model presents a different yet intriguing challenge—it has a Wiener-type structure featuring a linear dynamic subsystem in cascade with a static nonlinear subsystem. Although our work in [1] provides a parameter estimation scheme, it is limited to only constant charging or discharging protocols. Note of the existing methods is applicable here since they are designed for non-Wiener-type models. We are thus motivated to custom-develop an approach with an awareness of the NDC model's Wiener-like structure. Wiener system identification is an important subject in the area of system identification, which has seen a few methods proposed in the literature [26]. Among them, one of the most promising is based on the maximum likelihood (ML) estimation [27; 28]. However, the optimization procedure resulting from the ML formulation often suffers the issue of local minima, fundamentally blamed on the nonlinearity involved in the NDC model. If not addressed, this problem can easily lead to parameter estimates physically meaningless and useless when one applies the ML method to identifying the NDC model.

N. Tian and H. Fang are with the Department of Mechanical Engineering, University of Kansas, Lawrence, KS, 66045 USA {ning.tian@ku.edu, fang@ku.edu}.

Y. Wang is with the Mitsubishi Electric Research Laboratories, Cambridge, MA, 02139 USA {yebinwang@merl.com}.

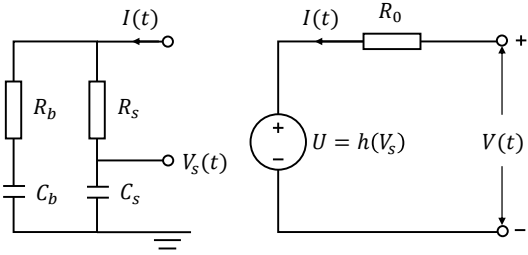


Fig. 1: Diagram of a nonlinear double-capacitor model.

Statement of contributions. Focused on the NDC model identification, this work offers three contributions. First, we propose to enable Wiener system identification based on maximum a posteriori (MAP) estimation. Compared to ML, MAP incorporates into the estimation design a prior distribution of the unknown parameters, which represents additional information or prior knowledge and can help drive the parameter search toward a physically reasonable parameter space. Second, based on the above notion, we systematically develop an MAP-based parameter identification approach for the NDC model. The proposed approach can estimate all the model parameters in just one shot and allows for almost arbitrary current profiles. Finally, we evaluate the approach using simulations and experiments, well validating validating its efficacy.

Organization. The rest of the paper is organized as follows. Section II reveals the Wiener-type structure underlying the NDC model. Inspired by Wiener system identification, Section III develops a new MAP-based parameter estimation approach to identify the NDC model. Section IV presents numerical simulation to assess the proposed approach, and further, experimental validation is offered in Section V. Finally, some concluding remarks are gathered in Section VI.

II. THE NDC MODEL

This section introduces the NDC model and further unveils its inherent Wiener-type architecture.

The NDC model is schematically shown in Figure 1. It is an extension of a linear double-capacitor model in [1] to account for a battery's nonlinear phenomena. Its first main part is two R-C circuits, i.e., C_b - R_b and C_s - R_s , which are configured in parallel. They are designed to imitate a battery's electrode. Specifically, C_b - R_b is analogous to the electrode's bulk inner part, and C_s - R_s corresponds to the surface region. The charge is stored in and migrates between C_b and C_s . This hence implies $C_b \gg C_s$, and $R_b \gg R_s$. The second part consists of a voltage source U and an internal resistance R_0 . Here, U is an analog to the OCV and based on a nonlinear mapping of V_s , i.e., $U = h(V_s)$. In addition, R_0 is included to mimic the electrolyte resistance. It is shown in [1] that this model provides excellent predictive capability for a battery's voltage behavior.

The dynamics of the NDC model can be characterized by

the following state-space model:

$$\begin{cases} \begin{bmatrix} \dot{V}_b(t) \\ \dot{V}_s(t) \end{bmatrix} = A \begin{bmatrix} V_b(t) \\ V_s(t) \end{bmatrix} + BI(t), \\ V(t) = h(V_s(t)) + R_0 I(t), \end{cases} \quad (1a)$$

where V_b and V_s are the voltages across C_b and C_s , respectively, I the current applied for charging ($I > 0$) or discharging ($I < 0$), V the terminal voltage, and

$$A = \begin{bmatrix} -\frac{1}{C_b(R_b+R_s)} & \frac{1}{C_b(R_b+R_s)} \\ \frac{1}{C_s(R_b+R_s)} & -\frac{1}{C_s(R_b+R_s)} \end{bmatrix}, \quad B = \begin{bmatrix} \frac{R_s}{C_b(R_b+R_s)} \\ \frac{R_b}{C_s(R_b+R_s)} \end{bmatrix}.$$

In addition, we parameterize $h(V_s)$ as a fifth-order polynomial:

$$h(V_s) = \beta_0 + \beta_1 V_s + \beta_2 V_s^2 + \beta_3 V_s^3 + \beta_4 V_s^4 + \beta_5 V_s^5,$$

where β_i for $i = 0, 1, \dots, 5$ are coefficients. Note that V_b and V_s should be set to belong to an interval $[V_s, \bar{V}_s]$, and for simplicity we let $\underline{V}_s = 0$ V and $\bar{V}_s = 1$ V. Then, $V_b = V_s = 1$ V for full charge (SoC = 100%), and $V_b = V_s = 0$ V for full depletion (SoC = 0%). In this work, we consider full discharging experiments to identify the model. That is, the initial V is \bar{V} that corresponds to the voltage at full charge, and the discharging ends when V hits the cut-off threshold \underline{V} . Then, we can obtain $\beta_0 = \underline{V}$ and $\sum_{i=1}^5 \beta_i = \bar{V}$. Furthermore, it can also be easily derived that OCV = $h(\text{SoC})$ holds [1].

Looking further at the NDC model, we can see that it has a structure akin to a Wiener system—the parallel R-C circuits constitute a linear dynamic subsystem, and cascaded with it is a static nonlinear mapping. Next, we convert (1) to a discrete-time Wiener-type formulation.

Applying zero-order-hold discretization to (1a) and the deriving the the transfer-function form, we have

$$V_s(t) = G_1(q)I(t) + G_2(q)V_s(0), \quad (2)$$

where

$$G_1(q) = \frac{\alpha_1 q^{-1} + \alpha_2 q^{-2}}{1 - (1 + \alpha_3)q^{-1} + \alpha_3 q^{-2}},$$

$$G_2(q) = \frac{1}{1 - q^{-1}},$$

with

$$\alpha_1 = \frac{A_{21}B_{11} + A_{12}B_{21}}{A_{12} + A_{21}} \Delta t$$

$$- \frac{A_{21}B_{11} - A_{21}B_{21}}{(A_{12} + A_{21})^2} \left(1 - e^{-(A_{12}+A_{21})\Delta t}\right),$$

$$\alpha_2 = -\frac{A_{21}B_{11} + A_{12}B_{21}}{A_{12} + A_{21}} e^{-(A_{12}+A_{21})\Delta t} \Delta t$$

$$+ \frac{A_{21}B_{11} - A_{21}B_{21}}{(A_{12} + A_{21})^2} \left(1 - e^{-(A_{12}+A_{21})\Delta t}\right),$$

$$\alpha_3 = e^{-(A_{12}+A_{21})\Delta t}.$$

Here, q^{-1} is the backshift operator, i.e., $q^{-1}s(t) = s(t-1)$ for a signal $s(t)$, and Δt the sampling period. It should be noted that only three parameters, α_i for $i = 1, 2, 3$ appear in (2), though (1a) involves four physical parameters, C_b , C_s ,

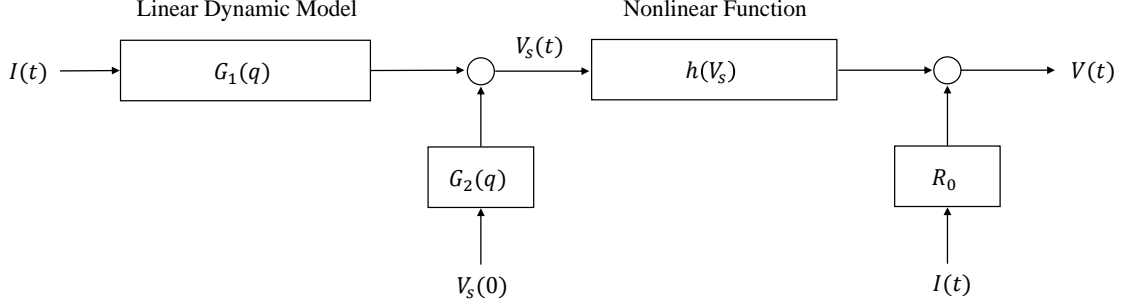


Fig. 2: The Wiener-type structure of the NDC model.

R_b and R_s . Hence, there is a redundancy for the physical parameters, which implies unidentifiability. To fix this issue, we let $R_s = 0$ following [17], because of the relatively less important role of R_s . Then, one can find out that

$$\begin{aligned}\alpha_1 &= \frac{\Delta t}{C_b + C_s} + \frac{R_b C_b^2}{(C_b + C_s)^2} (1 - \alpha_3), \\ \alpha_2 &= -\frac{\Delta t}{C_b + C_s} e^{-\frac{C_b + C_s}{C_b C_s R_b} \Delta t} - \frac{R_b C_b^2}{(C_b + C_s)^2} (1 - \alpha_3), \\ \alpha_3 &= e^{-\frac{C_b + C_s}{C_b C_s R_b} \Delta t}.\end{aligned}$$

If α_i for $i = 1, 2, 3$ are determined, we can easily reconstruct C_b , C_s and R_b as follows:

$$\begin{aligned}C_s &= \frac{(1 - \alpha_3)^2 \Delta t}{(\alpha_1 + \alpha_2)(1 - \alpha_3) + (\alpha_2 + \alpha_1 \alpha_3) \log \alpha_3}, \\ C_b &= \frac{(1 - \alpha_3) \Delta t}{\alpha_1 + \alpha_2} - C_s, \\ R_b &= -\frac{(\alpha_2 + \alpha_1 \alpha_3) (\Delta t^2)}{(\alpha_1 + \alpha_2)^2 C_b^2}.\end{aligned}$$

Finally, it is obvious that V is governed by

$$V(t) = h[G_1(q)I(t) + G_2(q)V_s(0)] + R_0 I(t). \quad (3)$$

With the above formulation, we have the block-oriented Wiener-type structure of the NDC model as depicted in Figure 2, in which the linear dynamic model $G_1(q)$ and the nonlinear function $h(V_s)$ are interconnected sequentially. Given this Wiener-type model, we wish to estimate all of its parameters simultaneously, including α_i for $i = 1, 2, 3$, β_i for $i = 1, 2, \dots, 4$ and R_0 , from the I - V data.

III. PARAMETER IDENTIFICATION

We address the NDC parameter identification from the Wiener perspective in this section. We build the solution on Bayesian MAP estimation.

Before proceeding further, we pose the following model based on (3):

$$y(t) = V(\boldsymbol{\theta}; u(t)) + v(t), \quad (4)$$

where u is the input current I , y the measured voltage, v the measurement noise added to V and assumed to follow a Gaussian distribution $\mathcal{N}(0, q)$, and

$$\begin{aligned}\boldsymbol{\theta} &= [\alpha_1 \ \alpha_2 \ \alpha_3 \ \beta_1 \ \beta_2 \ \beta_3 \ \beta_4 \ R_0]^\top, \\ V(\boldsymbol{\theta}; u(t)) &= h[G_1(q, \boldsymbol{\theta})u(t) + G_2(q)V_s(0), \boldsymbol{\theta}] + \theta_8 u(t).\end{aligned}$$

The input (current) and output (voltage) datasets are denoted as

$$\begin{aligned}\mathbf{y} &= [y_1 \ y_2 \ \cdots \ y_N]^\top, \\ \mathbf{u} &= [u_1 \ u_2 \ \cdots \ u_N]^\top,\end{aligned}$$

where N is the total number of sample instants. A combination of them is expressed as

$$\mathbf{Z} = [\mathbf{y} \ \mathbf{u}].$$

An ML-based approach is developed in [27] to deal with Wiener system identification. If applied to (4), it leads to consideration of the following problem:

$$\hat{\boldsymbol{\theta}} = \arg \max_{\boldsymbol{\theta}} p(\mathbf{Z} | \boldsymbol{\theta}).$$

Following this line, one can derive a likelihood cost function and find out the parameter estimates to minimize it. However, this method can be vulnerable to the risk of getting stuck of local minima because of the nonconvexity issue resulting from the static nonlinear function $h(\cdot)$. This can cause unphysical estimates. While carefully selecting an initial guess is suggested as a means to alleviate this problem [29], it may still not be adequate.

To overcome this problem, we propose to perform MAP estimation as it incorporates some prior knowledge to help drive the parameter search toward a reasonable minimum point. Specifically, we consider maximizing the *a posteriori* probability distribution of $\boldsymbol{\theta}$ conditioned on \mathbf{Z} :

$$\hat{\boldsymbol{\theta}} = \arg \max_{\boldsymbol{\theta}} p(\boldsymbol{\theta} | \mathbf{Z}). \quad (5)$$

Using the Bayes' theorem, we have

$$p(\boldsymbol{\theta} | \mathbf{Z}) = \frac{p(\mathbf{Z} | \boldsymbol{\theta}) p(\boldsymbol{\theta})}{p(\mathbf{Z})} \propto p(\mathbf{Z} | \boldsymbol{\theta}) \cdot p(\boldsymbol{\theta}). \quad (6)$$

TABLE I: A Quasi-Newton method for MAP estimation.

Data: current, voltage \mathbf{y} , prior knowledge \mathbf{m} and \mathbf{P} given initial iterate $\boldsymbol{\theta}_0$ and convergence tolerance ε

repeat

 compute the gradient vector \mathbf{g}_k

if $k = 0$ **then**

 set $\mathbf{H}_0 = 0.001 \frac{1}{\|\mathbf{g}_0\|} \mathbf{I}$

end if

if $k = 1$ **then**

 compute $\boldsymbol{\delta}_k = \boldsymbol{\theta}_k - \boldsymbol{\theta}_{k-1}$, $\boldsymbol{\gamma}_k = \mathbf{g}_k - \mathbf{g}_{k-1}$,

 set $\mathbf{H}_k = \frac{\boldsymbol{\delta}_k^\top \boldsymbol{\gamma}_k}{\boldsymbol{\gamma}_k^\top \boldsymbol{\gamma}_k} \mathbf{I}$

else

 set $\mathbf{H}_k = \left(\mathbf{I} - \frac{\boldsymbol{\delta}_k \boldsymbol{\gamma}_k^\top}{\boldsymbol{\delta}_k^\top \boldsymbol{\gamma}_k} \right) \mathbf{H}_{k-1} \left(\mathbf{I} - \frac{\boldsymbol{\gamma}_k \boldsymbol{\delta}_k^\top}{\boldsymbol{\delta}_k^\top \boldsymbol{\gamma}_k} \right) + \frac{\boldsymbol{\delta}_k \boldsymbol{\delta}_k^\top}{\boldsymbol{\delta}_k^\top \boldsymbol{\gamma}_k}$

end if

 compute $\mathbf{s}_k = -\mathbf{H}_k \mathbf{g}_k$

 assign $\lambda = 0.2$ and $c_1 = 10^{-6}$

if $J(\boldsymbol{\theta}_k + \lambda \mathbf{s}_k) \leq J(\boldsymbol{\theta}_k) + c_1 \lambda \mathbf{g}_k^\top \mathbf{s}_k$ **then**

 set $\boldsymbol{\theta}_{k+1} = \boldsymbol{\theta}_k + \lambda \mathbf{s}_k$

else

 assign $c_2 = 0.1$ and set $\boldsymbol{\theta}_{k+1} = \boldsymbol{\theta}_k + c_2 \lambda \mathbf{s}_k$

end if

until $J(\boldsymbol{\theta}_k)$ converged

return $\hat{\boldsymbol{\theta}} = \boldsymbol{\theta}_k$

In above, $p(\boldsymbol{\theta})$ quantifies the prior information available about $\boldsymbol{\theta}$. A general way is to characterize it as a Gaussian random vector following the distribution $p(\boldsymbol{\theta}) \sim \mathcal{N}(\mathbf{m}, \mathbf{P})$. Based on (4), $p(\mathbf{y}|\boldsymbol{\theta}) \sim \mathcal{N}(\mathbf{V}(\boldsymbol{\theta}, \mathbf{u}), \mathbf{Q})$, where $\mathbf{Q} = q\mathbf{I}$ and

$$\mathbf{V}(\boldsymbol{\theta}, \mathbf{u}) = [\mathbf{V}(\boldsymbol{\theta}, u(t_1)) \quad \dots \quad \mathbf{V}(\boldsymbol{\theta}, u(t_N))]^\top.$$

It then follows that

$$p(\mathbf{Z}|\boldsymbol{\theta}) \cdot p(\boldsymbol{\theta}) \propto \exp\left(-\frac{1}{2} [\mathbf{y} - \mathbf{V}(\boldsymbol{\theta}, \mathbf{u})]^\top \mathbf{Q}^{-1} \cdot [\mathbf{y} - \mathbf{V}(\boldsymbol{\theta}, \mathbf{u})]\right) \cdot \exp\left(-\frac{1}{2} (\boldsymbol{\theta} - \mathbf{m})^\top \mathbf{P}^{-1} (\boldsymbol{\theta} - \mathbf{m})\right).$$

Considering the log-likelihood, the problem formulated in (5) can be expressed as

$$\hat{\boldsymbol{\theta}} = \arg \max_{\boldsymbol{\theta}} J(\boldsymbol{\theta}), \quad (7)$$

where

$$J(\boldsymbol{\theta}) = \frac{1}{2} [\mathbf{y} - \mathbf{V}(\boldsymbol{\theta}, \mathbf{u})]^\top \mathbf{Q}^{-1} [\mathbf{y} - \mathbf{V}(\boldsymbol{\theta}, \mathbf{u})] + \frac{1}{2} (\boldsymbol{\theta} - \mathbf{m})^\top \mathbf{P}^{-1} (\boldsymbol{\theta} - \mathbf{m}).$$

One must resort to numerical optimization to solve (7). Here, we exploit a Quasi-Newton method [44] and introduce it briefly in the following for the sake of completeness. This method is premised on iteratively updating the parameter estimate, i.e.,

$$\boldsymbol{\theta}_{k+1} = \boldsymbol{\theta}_k + \lambda \mathbf{s}_k.$$

Here, λ denotes the step size, and \mathbf{s}_k the gradient-based search direction given by

$$\mathbf{s}_k = -\mathbf{B}_k \mathbf{g}_k,$$

where \mathbf{B}_k is a positive definite matrix that approximates the Hessian matrix $\nabla^2 J(\boldsymbol{\theta}_k)$, and $\mathbf{g}_k = \nabla J(\boldsymbol{\theta}_k)$. Based on [45], the iterative update of \mathbf{B}_k can be through

$$\mathbf{B}_k = \left(\mathbf{I} - \frac{\boldsymbol{\delta}_k \boldsymbol{\gamma}_k^\top}{\boldsymbol{\delta}_k^\top \boldsymbol{\gamma}_k} \right) \mathbf{B}_{k-1} \left(\mathbf{I} - \frac{\boldsymbol{\gamma}_k \boldsymbol{\delta}_k^\top}{\boldsymbol{\delta}_k^\top \boldsymbol{\gamma}_k} \right) + \frac{\boldsymbol{\delta}_k \boldsymbol{\delta}_k^\top}{\boldsymbol{\delta}_k^\top \boldsymbol{\gamma}_k},$$

with $\boldsymbol{\delta}_k = \boldsymbol{\theta}_k - \boldsymbol{\theta}_{k-1}$ and $\boldsymbol{\gamma}_k = \mathbf{g}_k - \mathbf{g}_{k-1}$. In addition, \mathbf{g}_k can be obtained as

$$\mathbf{g}_k = -\frac{\partial \mathbf{V}(\boldsymbol{\theta}_k, \mathbf{u})^\top}{\partial \boldsymbol{\theta}_k} \mathbf{Q}^{-1} [\mathbf{y} - \mathbf{V}(\boldsymbol{\theta}_k, \mathbf{u})] + \mathbf{P}^{-1} (\boldsymbol{\theta}_k - \mathbf{m}).$$

Specifically, each element in \mathbf{g} is given by

$$g_i = -\frac{2}{\sigma} \sum_{j=3}^N \eta_j \Sigma_j u(j-i) + \Lambda_i, \quad \text{for } i = 1, 2,$$

$$g_3 = -\frac{2}{\sigma} \sum_{j=3}^N \eta_j \Sigma_j \cdot (x_{j-1} - x_{j-2}) + \Lambda_3,$$

$$g_i = -\frac{2}{\sigma} \sum_{j=3}^N \eta_j (x_j^{i-3} - x_j^5) + \Lambda_i, \quad \text{for } i = 4, \dots, 7,$$

$$g_8 = -\frac{2}{\sigma} \sum_{j=1}^N \eta_j u(j) + \Lambda_8,$$

with

$$\eta_j = y_j - V(\boldsymbol{\theta}; u(t_j)),$$

$$x_j = G_1(q, \boldsymbol{\theta}) u(j) + G_2(q) V_s(0),$$

$$\Sigma_j = \sum_{i=4}^7 (i-3) \theta_i x_j^{i-1} + 5 \left(\bar{V} - \underline{V} - \sum_{i=4}^7 \theta_i \right) x_j^4,$$

$$\Lambda_i = \frac{2}{P_{ii}} (\theta_i - m_i).$$

Finally, note that λ needs to be chosen carefully to make $J(\boldsymbol{\theta})$ decrease monotonically. We can use the Armijo condition and let λ be selected such that

$$J(\boldsymbol{\theta}_k + \lambda \mathbf{s}_k) < J(\boldsymbol{\theta}_k) + c_1 \lambda \mathbf{g}_k^\top \mathbf{s}_k,$$

for some constant $c_1 \in (0, 1)$. In practice, c_1 is selected to be quite small, e.g., $c_1 = 10^{-6}$. To satisfy Armijo condition, a simple implementation is to start λ with a small value, say $\lambda = 0.2$. If the Armijo condition is not met, reduce λ and proceed further. Summarizing the above, we outline the computational algorithm in Table I.

Remark 1: The proposed approach requires some prior knowledge of the parameters to be available. One can develop such a prior knowledge in several ways in practice. First, R_0 can be roughly estimated using the voltage drop at the beginning of the discharge, to which it is a main contributor. Second, the polynomial coefficients of $h(\cdot)$ can be approximately obtained from an experimentally calibrated

SoC-OCV curve. Third, one can derive a rough range for $C_b + C_s$ if a battery's capacity is approximately known. Finally, as the parameters of batteries of the same kind and brand are usually close, one can use the parameter estimates obtained from one battery as prior knowledge for another.

IV. NUMERICAL SIMULATION

This section offers a numerical example to evaluate the efficacy of the identification method proposed in Section III.

Consider a battery with $C_b = 10,101$ F, $C_s = 1,277$ F, $R_b = 39.73$ m Ω , $R_s = 0$ m Ω , $R_0 = 80$ m Ω , and

$$h(V_s) = 3.2 + 2.586 \cdot V_s - 9.024 \cdot V_s^2 + 18.88 \cdot V_s^3 - 17.84 \cdot V_s^4 + 6.358 \cdot V_s^5.$$

Suppose that the battery is initially at full charge with the terminal voltage equal to the upper threshold $\bar{V} = 4.16$ V. It is then discharged until hitting the lower cut-off threshold $\underline{V} = 3.2$ V, respectively. The discharging current profile is based on the Urban Dynamometer Driving Schedule (UDDS) [?] and adjusted to fall between 0 A and 6 A, see Figure 3(a). The sampling period $\Delta t = 1$ s, and the Gaussian measurement noise has mean of 0 and covariance of 10^{-4} .

For simulation, the proposed identification approach is applied to synthetic data generated in the above setting. The simulation is run for $M = 100$ times to make a fair evaluation. In each run, the initial parameter guess is given in Table II. We use only the prior knowledge about α_1 through α_3 and set \mathbf{m} and \mathbf{P} accordingly as shown in Table II. Two metrics are considered to evaluate the estimation accuracy:

$$\bar{\theta}_i = \frac{1}{M} \sum_{j=1}^M \hat{\theta}_i(j),$$

$$\sigma_{r,i} = \sqrt{\frac{\frac{1}{M} \sum_{j=1}^M (\hat{\theta}_i(j) - \theta_i)^2}{\theta_i^2}},$$

for $i = 1, 2, \dots, 8$, which represents the average estimate and estimation error, respectively. The results obtained from the simulation runs are also summarized in Table II. It is seen that there is a close match between the parameter estimates and the true value, showing the effectiveness of the proposed identification approach. We further show the reconstruction of C_b , C_s and R_b in III. It is observed that their estimates match the truth with high accuracy. Besides, Figure 3(b) offers a comparison between measured and predictive voltage in simulation run, which illustrates an excellent predictive accuracy.

V. EXPERIMENTAL VALIDATION

This section evaluates the effectiveness of the identification approach in the real-world application.

Our experiments were conducted on a PEC[®] SBT4050 battery tester. Using this facility, charging/discharging tests were performed on a Panasonic NCR18650B Li-ion battery cell, which has a rated capacity of 3.25 Ah. In one test, the battery was discharged from full capacity by the UDDS

current profile depicted in Figure 3(a). The obtained voltage profile is shown in Figure 4 (see the red curve). The sampling time interval Δt was 1 s, and the cut-off voltage \bar{V} is 3.2 V. We applied the proposed approach to the collected current/voltage data to identify the parameters. The initial guess, selected \mathbf{m} and \mathbf{P} , and the obtained parameter estimates are summarized in Table IV¹. Here, the initial guess and prior knowledge understandably play an important role in the estimation accuracy. To sensibly obtain them, we run the method in [1] to make an approximate estimation first. The voltage prediction is made using the parameter estimates and compared against the measured voltage in Figure 4. One can observe an excellent agreement between them. In addition, it will be interesting to compare the estimated SoC-OCV curve with the true one of the battery. As aforementioned, $\text{OCV} = h(\text{SoC})$ for the NDC model. It is identified here as

$$\text{OCV} = 3.2 + 2.586 \cdot \text{SoC} - 9.024 \cdot \text{SoC}^2 + 18.88 \cdot \text{SoC}^3 - 17.84 \cdot \text{SoC}^4 + 6.358 \cdot \text{SoC}^5.$$

Figure 5 compares it with the SoC-OCV curve obtained experimentally by discharging the battery from full capacity to a cut-off voltage 3.2 V using a small current of 0.1 A. It is seen that the identified SoC-OCV curve is very close to the actual one. All the results above show the parameter estimates are reasonable and that the identification method introduced in Section IV is effective.

VI. CONCLUSION

This paper deals with parameter identification for the NDC model proposed in our previous work. The NDC model is structurally similar to a Wiener system as it consists of a linear dynamic subsystem and a nonlinear static subsystem in cascade. Known as a challenging problem, Wiener system identification can often easily fall victim to nonconvexity and local minima due to the model's nonlinearity. To address this issue, we proposed to use MAP estimation so as to incorporate some prior knowledge about the unknown parameters into the design of parameter estimation. Based on this idea, we developed a parameter estimation approach for the NDC model. We validated the approach through simulation and experiments, consistently observing its effectiveness in producing accurate estimation. The proposed approach can advantageously estimate all the model parameters in one shot, imposes no restrictions on the current profiles, and are more capable of ensuring physically reasonable estimates to be obtained. The notion of MAP-based Wiener system identification can also find prospective use in many other applications.

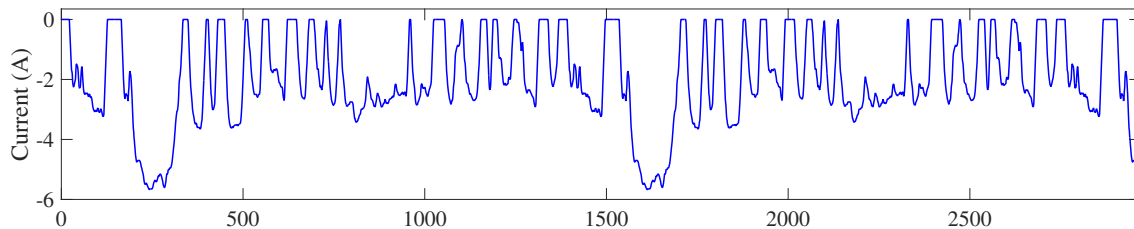
REFERENCES

- [1] N. Tian, H. Fang, and J. Chen, "A new nonlinear double-capacitor model for rechargeable batteries," in *Industrial Electronics Society, IECON 2018-44th Annual Conference of the IEEE*. IEEE, 2018, in press.
- [2] B. Schweighofer, K. M. Raab, and G. Brasseur, "Modeling of high power automotive batteries by the use of an automated test system,"

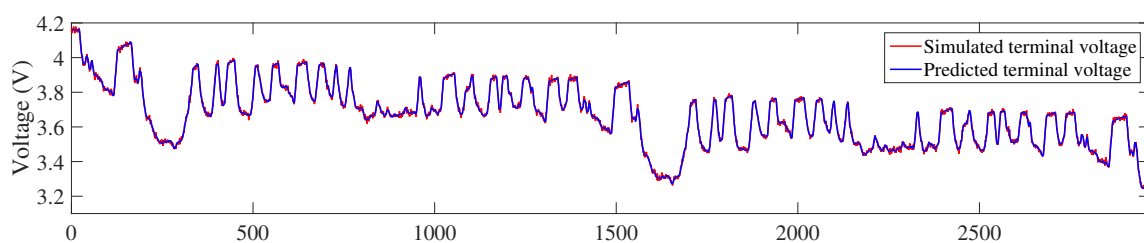
¹Note that the battery parameters for simulation in Section IV are indeed based on the estimation results here to make the simulation more realistic.

TABLE II: Parameter identification results from Monte Carlo simulation.

Name	α_1	α_2	α_3	β_1	β_2	β_3	β_4	R_0
θ	7.7552×10^{-4}	-7.7359×10^{-4}	0.97804	2.586	-9.024	18.88	-17.84	0.08
m	7.7552×10^{-4}	-7.7359×10^{-4}	0.97804	-	-	-	-	0.08
diag(P)	$(0.15 \times m_1)^2$	$(0.15 \times m_2)^2$	$(0.15 \times m_3)^2$	-	-	-	-	$(0.1 \times m_8)^2$
θ	7.7378×10^{-4}	-7.7185×10^{-4}	0.97804	2.586	-9.024	18.88	-17.84	0.08
σ_r (%)	0.3	0.3	1.4×10^{-6}	1×10^{-4}	1.5×10^{-5}	6×10^{-6}	5×10^{-6}	7×10^{-3}



(a) Variable currents.



(b) Comparison between simulated terminal voltage and predicted voltage.

Fig. 3: Validation based on one Monte-Carlo simulation results.

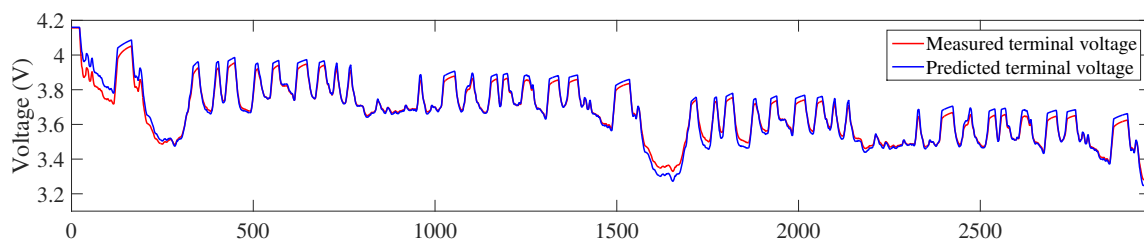


Fig. 4: Comparison between measured terminal voltage and predicted terminal voltage.

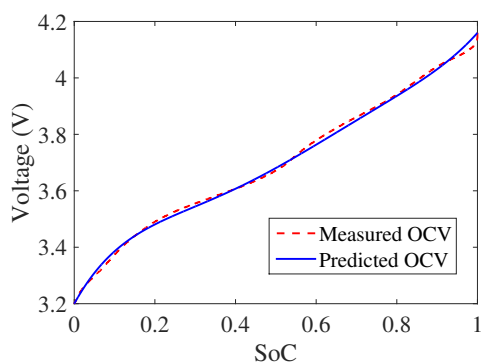


Fig. 5: Comparison between measured and predicted OCV.

TABLE III: Parameter identification results of C_b , C_s and R_b from Monte Carlo simulation.

Name	C_b	C_s	R_s
Real	10, 101	1, 277	0.03973
Sample mean	10, 088	1, 280	0.03966
Relative sample deviation (%)	0.2	0.32	0.26

IEEE Transactions on Instrumentation and Measurement, vol. 52, no. 4, pp. 1087–1091, 2003.

- [3] S. Abu-Sharkh and D. Doerffel, “Rapid test and non-linear model characterisation of solid-state lithium-ion batteries,” *Journal of Power Sources*, vol. 130, no. 1, pp. 266–274, 2004.
- [4] A. Fairweather, M. Foster, and D. Stone, “Battery parameter identification with Pseudo Random Binary Sequence excitation (PRBS),” *Journal of Power Sources*, vol. 196, no. 22, pp. 9398–9406, 2011.
- [5] M. Dubarry and B. Y. Liaw, “Development of a universal modeling tool for rechargeable lithium batteries,” *Journal of Power Sources*, vol. 174, no. 2, pp. 856–860, 2007.
- [6] H. He, R. Xiong, X. Zhang, F. Sun, and J. Fan, “State-of-charge estimation of the lithium-ion battery using an adaptive extended Kalman filter based on an improved Thevenin model,” *IEEE Transactions on Vehicular Technology*, vol. 60, no. 4, pp. 1461–1469, 2011.
- [7] Y. Tian, B. Xia, W. Sun, Z. Xu, and W. Zheng, “A modified model

TABLE IV: Parameter identification results from experimental current/voltage data.

Name	α_1	α_2	α_3	β_1	β_2	β_3	β_4	R_0
θ_{guess}	6.5×10^{-4}	-6.48×10^{-4}	0.9776	2.59	-9.003	18.87	-17.82	0.07
\mathbf{m}	6.5×10^{-4}	-6.48×10^{-4}	0.9776	-	-	-	-	0.07
$\text{diag}(\mathbf{P})$	$(0.15 \times m_1)^2$	$(0.15 \times m_2)^2$	$(0.15 \times m_3)^2$	-	-	-	-	$(0.1 \times m_8)^2$
$\hat{\theta}$	7.7552×10^{-4}	-7.7359×10^{-4}	0.97804	2.586	-9.024	18.88	-17.84	0.08

based state of charge estimation of power lithium-ion batteries using unscented Kalman filter,” *Journal of Power Sources*, vol. 270, pp. 619–626, 2014.

- [8] P. Mauracher and E. Karden, “Dynamic modelling of lead/acid batteries using impedance spectroscopy for parameter identification,” *Journal of Power Sources*, vol. 67, no. 1-2, pp. 69–84, 1997.
- [9] K. Goebel, B. Saha, A. Saxena, J. R. Celaya, and J. P. Christophersen, “Prognostics in battery health management,” *IEEE Instrumentation & Measurement Magazine*, vol. 11, no. 4, 2008.
- [10] C. Birkl and D. Howey, “Model identification and parameter estimation for LiFePO₄ batteries,” in *Proceedings of IET Hybrid and Electric Vehicles Conference*, 2013, pp. 1–6.
- [11] T. Hu and H. Jung, “Simple algorithms for determining parameters of circuit models for charging/discharging batteries,” *Journal of Power Sources*, vol. 233, pp. 14–22, 2013.
- [12] Z. He, G. Yang, and L. Lu, “A parameter identification method for dynamics of lithium iron phosphate batteries based on step-change current curves and constant current curves,” *Energies*, vol. 9, no. 6, p. 444, 2016.
- [13] J. Yang, B. Xia, Y. Shang, W. Huang, and C. Mi, “Improved battery parameter estimation method considering operating scenarios for HEV/EV applications,” *Energies*, vol. 10, no. 1, p. 5, 2016.
- [14] N. Tian, Y. Wang, J. Chen, and H. Fang, “On parameter identification of an equivalent circuit model for lithium-ion batteries,” in *IEEE Conference on Control Technology and Applications*, 2017, pp. 187–192.
- [15] T. Feng, L. Yang, X. Zhao, H. Zhang, and J. Qiang, “Online identification of lithium-ion battery parameters based on an improved equivalent-circuit model and its implementation on battery state-of-power prediction,” *Journal of Power Sources*, vol. 281, pp. 192–203, 2015.
- [16] G. K. Prasad and C. D. Rahn, “Model based identification of aging parameters in lithium ion batteries,” *Journal of Power Sources*, vol. 232, pp. 79–85, 2013.
- [17] M. Sitterly, L. Y. Wang, G. G. Yin, and C. Wang, “Enhanced identification of battery models for real-time battery management,” *IEEE Transactions on Sustainable Energy*, vol. 2, no. 3, pp. 300–308, 2011.
- [18] Y. Hu and S. Yurkovich, “Linear parameter varying battery model identification using subspace methods,” *Journal of Power Sources*, vol. 196, no. 5, pp. 2913–2923, 2011.
- [19] Y. Li, C. Liao, L. Wang, L. Wang, and D. Xu, “Subspace-based modeling and parameter identification of lithium-ion batteries,” *International Journal of Energy Research*, vol. 38, no. 8, pp. 1024–1038, 2014.
- [20] J. C. Forman, S. J. Moura, J. L. Stein, and H. K. Fathy, “Genetic identification and fisher identifiability analysis of the Doyle–Fuller–Newman model from experimental cycling of a LiFePO₄ cell,” *Journal of Power Sources*, vol. 210, pp. 263 – 275, 2012.
- [21] L. Zhang, L. Wang, G. Hinds, C. Lyu, J. Zheng, and J. Li, “Multi-objective optimization of lithium-ion battery model using genetic algorithm approach,” *Journal of Power Sources*, vol. 270, pp. 367–378, 2014.
- [22] M. A. Rahman, S. Anwar, and A. Izadian, “Electrochemical model parameter identification of a lithium-ion battery using particle swarm optimization method,” *Journal of Power Sources*, vol. 307, pp. 86–97, 2016.
- [23] Z. Yu, L. Xiao, H. Li, X. Zhu, and R. Huai, “Model parameter identification for lithium batteries using the coevolutionary particle swarm optimization method,” *IEEE Trans. Ind. Electron.*, vol. 64, no. 7, pp. 5690–5700, 2017.
- [24] M. J. Rothenberger, D. J. Docimo, M. Ghanaatpishe, and H. K. Fathy, “Genetic optimization and experimental validation of a test cycle that maximizes parameter identifiability for a li-ion equivalent-circuit battery model,” *Journal of Energy Storage*, vol. 4, pp. 156 – 166, 2015.
- [25] S. Park, D. Kato, Z. Gima, R. Klein, and S. Moura, “Optimal input design for parameter identification in an electrochemical Li-ion battery model,” in *Proceedings of American Control Conference*, 2018, pp. 2300–2305.
- [26] F. Giri and E.-W. Bai, *Block-oriented nonlinear system identification*. Springer, 2010, vol. 1.
- [27] A. Hagenblad, L. Ljung, and A. Wills, “Maximum likelihood identification of Wiener models,” *Automatica*, vol. 44, no. 11, pp. 2697 – 2705, 2008.
- [28] L. Vanbeylen, R. Pintelon, and J. Schoukens, “Blind maximum-likelihood identification of wiener systems,” *IEEE Transactions on Signal Processing*, vol. 57, no. 8, pp. 3017–3029, 2009.
- [29] A. Hagenblad, “Aspects of the identification of Wiener models,” Ph.D. dissertation, Linköping University, 1999.
- [30] M. A. Roscher and D. U. Sauer, “Dynamic electric behavior and open-circuit-voltage modeling of LiFePO₄-based lithium ion secondary batteries,” *Journal of Power Sources*, vol. 196, no. 1, pp. 331–336, 2011.
- [31] R. Xiong, X. Gong, C. C. Mi, and F. Sun, “A robust state-of-charge estimator for multiple types of lithium-ion batteries using adaptive extended Kalman filter,” *Journal of Power Sources*, vol. 243, pp. 805–816, 2013.
- [32] E. Namor, D. Torregrossa, R. Cherkaoui, and M. Paolone, “Parameter identification of a lithium-ion cell single-particle model through non-invasive testing,” *Journal of Energy Storage*, vol. 12, pp. 138–148, 2017.
- [33] B. Xia, X. Zhao, R. De Callafon, H. Garnier, T. Nguyen, and C. Mi, “Accurate lithium-ion battery parameter estimation with continuous-time system identification methods,” *Applied Energy*, vol. 179, pp. 426–436, 2016.
- [34] Z. Deng, H. Deng, L. Yang, Y. Cai, and X. Zhao, “Implementation of reduced-order physics-based model and multi-parameters identification strategy for lithium-ion battery,” *Energy*, vol. 138, pp. 509–519, 2017.
- [35] Y. Cui, P. Zuo, C. Du, Y. Gao, J. Yang, X. Cheng, Y. Ma, and G. Yin, “State of health diagnosis model for lithium ion batteries based on real-time impedance and open circuit voltage parameters identification method,” *Energy*, vol. 144, pp. 647–656, 2018.
- [36] R. Xiong, F. Sun, X. Gong, and C. Gao, “A data-driven based adaptive state of charge estimator of lithium-ion polymer battery used in electric vehicles,” *Applied Energy*, vol. 113, pp. 1421–1433, 2014.
- [37] S. Yuan, L. Jiang, C. Yin, H. Wu, and X. Zhang, “A transfer function type of simplified electrochemical model with modified boundary conditions and padé approximation for Li-ion battery: Part 2. Modeling and parameter estimation,” *Journal of Power Sources*, vol. 352, pp. 258–271, 2017.
- [38] J. Sabatier, M. Aoun, A. Oustaloup, G. Grégoire, F. Ragot, and P. Roy, “Fractional system identification for lead acid battery state of charge estimation,” *Signal processing*, vol. 86, no. 10, pp. 2645–2657, 2006.
- [39] B. Wang, S. E. Li, H. Peng, and Z. Liu, “Fractional-order modeling and parameter identification for lithium-ion batteries,” *Journal of Power Sources*, vol. 293, pp. 151–161, 2015.
- [40] J. C. Forman, S. J. Moura, J. L. Stein, and H. K. Fathy, “Genetic parameter identification of the Doyle–Fuller–Newman model from experimental cycling of a LiFePO₄ battery,” in *American Control Conference (ACC), 2011*. IEEE, 2011, pp. 362–369.
- [41] N. Tian, Y. Wang, J. Chen, and H. Fang, “On parameter identification of an equivalent circuit model for lithium-ion batteries,” in *Control Technology and Applications (CCTA), 2017 IEEE Conference on*. IEEE, 2017, pp. 187–192.
- [42] A. Hagenblad, *Aspects of the identification of Wiener models*. Cite-seer, 1999.
- [43] L. Ljung and T. Chen, “What can regularization offer for estimation of dynamical systems?” in *11th IFAC International Workshop on Adaptation and Learning in Control and Signal Processing (ALCOSP13)*,

- 3-5 July 2013, Caen, France. IFAC, 2013, pp. 1–8.
- [44] A. Hagenblad, L. Ljung, and A. Wills, “Maximum likelihood identification of Wiener models,” *Automatica*, vol. 44, no. 11, pp. 2697–2705, 2008.
- [45] S. Wright and J. Nocedal, “Numerical optimization,” *Springer Science*, vol. 35, no. 67-68, p. 7, 1999.